Computational Materials Science 62 (2012) 276–281

Contents lists available at SciVerse ScienceDirect

Computational Materials Science

journal homepage: www.elsevier.com/locate/commatsci

How to minimise thermal fatigue in surface multi-treatments and coatings?

Pierre D'Ans *, Marc Degrez

Université Libre de Bruxelles (ULB), Ecole Polytechnique de Bruxelles, 4MAT Department, 50, Avenue F.D. Roosevelt, CP194/3, 1050 Bruxelles, Belgium

ARTICLE INFO

Article history:
Received 1 February 2012
Received in revised form 23 April 2012
Accepted 1 May 2012
Available online 4 June 2012

Keywords:
Surface treatments
Physical vapour deposition
Thermal spray
Thermal fatigue
Performance indices

ABSTRACT

A tool is developed to rank surface treated materials with respect to thermal fatigue. It comprises a modelling of the temperature profile in the component and an adaptation of the Coffin–Manson model for surface treatments fatigue. It is used as a performance index and discussed onto several surface treatments and multi-treatments relevant for the protection of steel in aluminium foundry moulds, exposed to thermal fatigue, with some insight in the effect of surface treatments processes on the final result. The model reproduces the well-known capability of duplex PVD nitride onto nitriding to withstand thermal fatigue. Using thermal barrier coatings may also be relevant, but the internal stress must be sufficiently compressive to be resistant to the studied thermal cycles.

1. Introduction

Thermal stresses affect materials in many fields: aircrafts engines, foundry devices affected by moulding cycles, turbine blades for the energy industry, nuclear fusion reactors, etc. When applied cyclically or repeatedly over time, they often lead to thermal fatigue. For applications involving surface treated metals, such stresses arise from a combination of several factors:

1. The difference of the thermal expansion coefficients of the surface layer and the substrate.
2. The thermal gradients during thermal transients.
3. The residual stresses due to the surface treatment process itself, still present at uniform ambient temperature.

Contributions 1 and 3 mainly affect the layers. Contribution 2 affects both the substrate and the treatment layers.

Frequently, literature provides with extensive and successful mathematical descriptions of thermal flows in multi-materials [1] and crack propagations at failure for specific coatings categories [2]. Some works focus on modelling the thermal fatigue of the substrate [3,4]. Several simple bulk thermal fatigue cases (contribution 2) were modelled in Manson's work [5], whereas modelling at least one contribution is presented elsewhere [6–10].

However, literature provides with very limited tools to compare coatings with totally different characteristics in terms of thermal fatigue lifetime for contributions 1–3. Such a semi-quantitative tool would be useful for designers to help to minimise the experimental investigations in thermal fatigue problems. The goal of this paper is to propose a way to fill this gap, by:

- Encompassing contributions 1–3 for single or multiple surface treatments.
- Using as much as possible parameters that can be found in the literature, instead of additional empirical parameters.

Surface treatments used for the aluminium die-casting operations are considered as a study case, since these treatments originate from different technologies and since the knowledge in this field is still quite empirical. Thermal fatigue acts there as a major failure mode for steel and its corrosion/sliding wear protective layers. Various treatments were compared: treatments aimed at reducing fatigue (nitriding [11–16], shot peening [17]), corrosion by molten aluminium (thin TiN coating [18–21], boriding [22–24]), and thermal gradients in the substrate (thin PVD thermally insulating oxide [25], thick zirconia [26] using plasma spray).

This paper first describes the model and the specific study case. Then, various surface treatments are ranked in terms of lifetimes in thermal cycling (with mechanical failure). A comparison is made with some important experimental results from the surface treatments literature.

2. Theory and calculation

The (x,y,z) Cartesian axis system sketched in Fig. 1 is assumed in the case of a double layer treatment. The studied treatments are represented in Fig. 2. The studied object is a 4 cm thick flat

* Corresponding author. Tel.: +32 (0)2 650 30 28; fax: +32 (0)2 650 27 86.
E-mail addresses: pdans@ulb.ac.be (P. D'Ans), mdegrez@ulb.ac.be (M. Degrez).

0927-0256/$ - see front matter © 2012 Elsevier B.V. All rights reserved.
http://dx.doi.org/10.1016/j.commatsci.2012.05.010

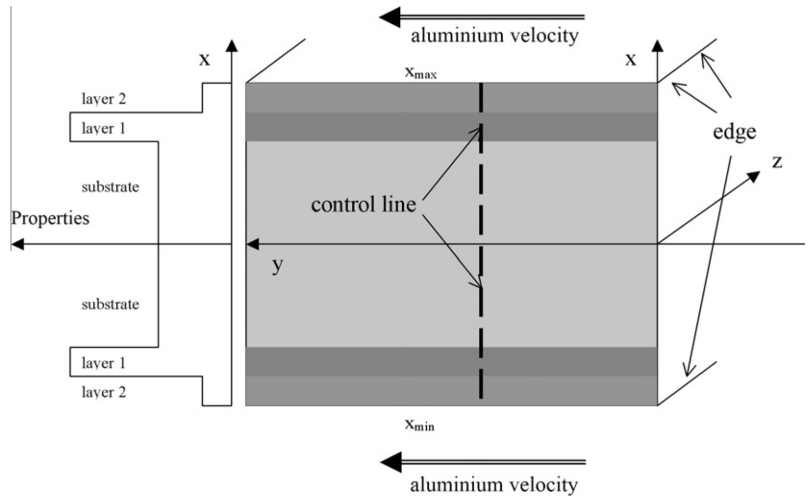

Fig. 1. Axis and properties definition (cross-section of the studied object).

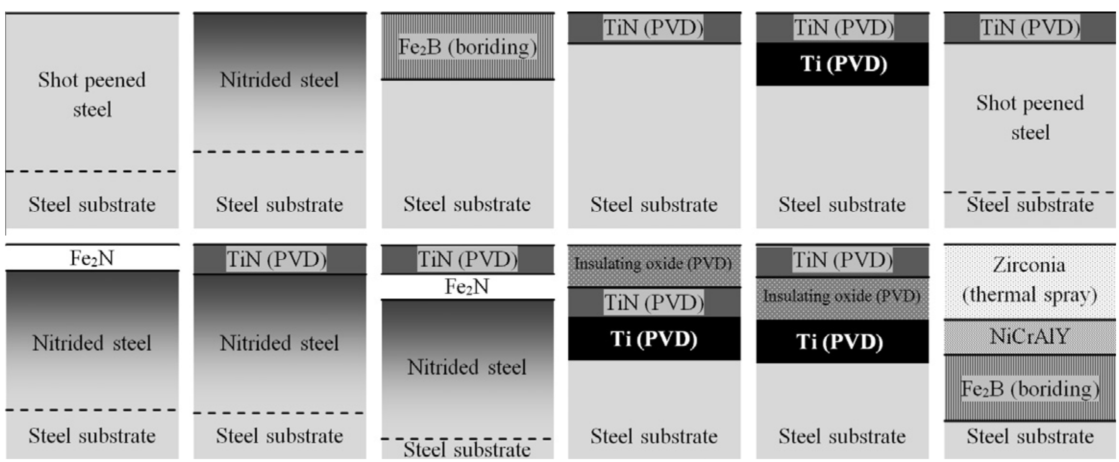

Fig. 2. Studied treatments.

semi-infinite plate, parallel to the y and z axis, symmetric with respect to the (y,z) plane. Such a simple geometry is used for a ranking purpose, but a more complex geometry can be used to model a complete mould during aluminium casting operations, for instance, to determine where failure occurs first.

The proposed methodology is based on the equations used in [27]. For a ranking purpose, it splits into the 9 following steps:

1. Definition of the studied surface treated material: substrate, surface treatment(s) and their respective thickness.
2. Definition of the cyclic time-dependent thermal boundary conditions.
3. For each material/treatment, data mining for: thermal expansion coefficient α, Young's modulus E, Poisson's modulus υ, ultimate strain ε_u, ultimate stress σ_u, specific heat C_p, density ρ, thermal conductivity k.

One further assumes that:

– The interfaces between the layers are flat and chemically stable.
– The materials properties are constant within a layer, as illustrated on the left-hand side of Fig. 1. In the cases of nitriding and shot peening, the actual layer is virtually sliced into thinner layers so that this assumption is acceptable within each of these. In the case of diffusion layers, several compound layers are sometimes obtained. They should be considered as distinct materials with distinct properties.

4. Define the process stresses σ_0 of each layer (biaxial along y and z). In the case of a thin enough coating, a uniform value is assumed along x. For deep treatments, a complex stress profile has to be assumed (think about shot peening, which generates compressive stress around the surface and tensile stress deeper; the same stands for the diffusion case of nitriding). It was then split into thin layers, each of which having a different value of σ_0.
5. Resolution of time-dependent heat transfer problem. The heat flow is assumed to be oriented along x, so that the 1-D Fourier equation has to be solved. Variable space and time integration steps are recommended, so that the space steps are shorter in the layers and their immediate surroundings. The time steps should also be shorter around the most important temperature changes.
6. For each time step, determination of the stress at each point of the treated layers and substrate: $\sigma(x,t)$ (t: time) in the one-dimension case. For each material, a stress–strain relationship is assumed. In this work, the materials were assumed either perfectly plastic or perfectly brittle, as sketched on Fig. 3. The stresses are biaxial along y and z

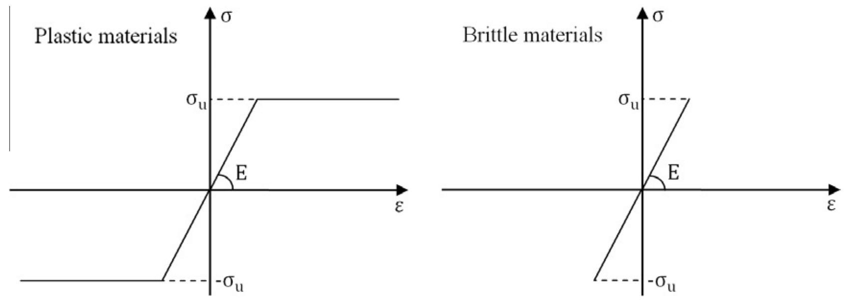

Fig. 3. Single load stress–strain behaviour of the studied materials.

and vary along x. No momentum balance was made, thanks to symmetry.

7. Determination of the corresponding mechanical strain $\varepsilon(x,t)$, defined in the same way as in [27]:

$$\varepsilon(x,t) = \varepsilon_0(x) + \varepsilon_{\text{average}}(t) - \varepsilon_{\text{th}}(x,t),$$

where the free thermal deformation of each element of the substrate or the layers, $\varepsilon_{\text{th}}(x,t) = \alpha(x)\Delta T(x,t)$, is prevented by the mechanical strain of the other elements, $\varepsilon_{\text{average}}$, and where ε_0 is the initial deformation of the layer, due to deposition stress.

8. At each space step, determination of the average stress $\bar{\sigma}(x,t)$ and the strain amplitude $\Delta\varepsilon(x,t)$.
9. Determination of the number of reversals at failure (lifetime, N_f) solving the following equations for N_f at each point of the material:

For ductile materials (metals, borides):

$$\Delta\varepsilon = 3.5\frac{\sigma_u - \bar{\sigma}}{E}N_f^{-0.12} + \varepsilon_u^{0.6}N_f^{-0.6} \quad (1)$$

For brittle materials (oxide, nitride layers):

$$\Delta\varepsilon = \frac{9}{4}\frac{\sigma_u - \bar{\sigma}}{E}N_f^{-0.083} \quad (2)$$

These equations have the form of the well-known Coffin–Manson equations [5]. They are chosen because they only need parameters that can be often found in literature and because they are valid for a wide range of materials, as shown in [27]. N_f is then used as a ranking index, to compare materials in a given context. The minimum value of N_f is considered as the lifetime of the whole component. Steps 5 to 9 were automatically implemented on MATLAB. The final temperature profile is generally different from the initial one, since several cycles are often necessary to achieve a limit cycle. Therefore, since high N_f values are expected, steps 5 to 9 can be repeated until such a limit cycle is reached [27].

For foundry moulds for aluminium, the boundary conditions are defined as follows:

– For the heating half cycle, the aluminium is assumed to move along the y axis (in Fig. 1, "aluminium velocity" represents the casting speed). The studied part is denoted by a vertical dotted line ("control line"), with a corresponding y value (distance from the edge). The heat transfer coefficient h is calculated along this line using the following relationship between the Prandtl number Pr, the Nusselt number Nu_y and the Reynold's number Re_y [27,28]:

$$Nu_y := h(y,U)y/k_{\text{fluid}} = 0.53\text{Pr}^{0.5}\text{Re}_y^{0.5}, \quad (3)$$

where U is the aluminium velocity. Since Eq. (3) can be applied for a Peclet number comprised between 10^2 and 10^4, the following assumptions are made: U = 10 m/s and y is fixed at 2 cm. The aluminium is at 1100 K outside the boundary layer.

– For the cooling half cycle (ejection of the moulding part and injection of cold lubricating fluid), it is assumed that h = 2500 W/m^2 K and that the ambient temperature is 293 K.

3. Results and discussion

Materials properties used for the calculations were borrowed from literature and are summarised in Table 1. In particular:

Table 1
Numerical values used for modelling. (See below-mentioned references for further information.)

Properties	H13	Ti (PVD)	TiN (PVD)	Insulating oxide (PVD)	White layer (nitriding)	Fe_2B (boriding)*	NiCrAlY (thermal spray)*	Zirconia (thermal spray)*
C_p (J/kg K)	608*	602 [32]	792 [32]	406 [32]	600 (Section 3)	651	$\frac{k}{C_p\rho} = 1.70 \times 10^{-6}$ m^2/s	609
k (W/km)	30*	22 [25]	22,5 [25]	0,69 [25]	30 (Section 3)	30		1.1
ρ (kg/m^3)	7600*	4500 [38]	5220 [38]	7650 [38]	6350 [39]	7430		5582
α (°C^{-1})	13.2×10^{-6}*	10.1×10^{-6} [25]	7.48×10^{-6} [25]	9.05×10^{-6}[25]	10.8×10^{-6} [33]	8.55×10^{-6}	16.55×10^{-6}	10.67×10^{-6}
E (GPa)	140	Not used***	424 [40]	Not used***	300 [41]	433	25	$\frac{\sigma_u}{E} = 0.0061$
σ_u (MPa)	600		5000 [40]		3000 [35]	400	Not used***	
ε_u	0.2		Brittle	Brittle	Brittle	0.02	Not used***	Brittle
υ	0.30*		0.2 [40]	0.2**	0.30 [41]	0.30	0.25	0
σ_0 (GPa)	See Section 3		0	0**	0,95 [41]	−2.51	0	0
Thickness (m)	0.02 × 2	0.5×10^{-6}	2,5 10^{-6}	10 10^{-6}	20×10^{-6}	40×10^{-6}	20×10^{-6}	150×10^{-6}

* See [36] for details.
** Assumption.
*** Assumed not to initiate rupture.

– Steel mechanical properties were considered at 873 K.
– The properties of Ti, TiN and the insulating oxide were taken from [25]. C_p is an average in the temperature range [373 K, 973 K], obtained from the available correlations. The insulating oxide was supposed to be CeO_2.
– For the nitriding compound layer, the k value was derived from the thermal diffusivity given in [29]. Typically, it contains Fe_2N (most stable compound at high temperature) or Fe_4N. C_p was obtained using the available correlations and averaging them on [300 K, 1000 K] for both compounds. Correlations from [30–32] give similar results. α was taken from another work dedicated to foundry, where plane stresses were also evaluated [33].

In the absence of nitriding or shot peening, $\sigma_0 = 0$ in the steel substrate. If such a treatment is applied, refer to Table 2 for the initial stress profile. The total thickness remains 2 cm $\times$ 2 in the case of shot peening, boriding or nitriding without any compound layer.

Table 3 shows the calculated values of N_f for all the studied treatments with the above mentioned values of the parameters ("default" parameters), in italics. In some cases, one also addresses the effect of changing these parameters (white boxes).

In the case of untreated steel, the thermal cycle is given in Fig. 4. Note that T hardly fluctuates at the centre of the object ($x = 0$), compared to the boundary ($x = 0.02$ m). Fig. 5 gives the corresponding superficial strains (i.e. at $x = 0.02$ m).

Italicised values for N_f in Table 3 represent a kind of "ranking parameter" of multi-materials and their manufacture process with respect to thermal fatigue. Besides, the obtained values typically represent practical values for numbers of shots at rupture, in the presence of surface treatments for foundry applications. However, directly extrapolating these results to "real-life" is less evident, owing to the very simplified geometry.

Using these default parameters, three types of situations arise:

– The treatment reduces N_f, like for the multilayer zirconia/NiCrAlY/boriding.
– The treatment hardly affects N_f, like for boriding or thin coatings. The latter case is in good agreement with the qualitative results of Y. Wang obtained with thin PVD nitride [19].
– The treatment improves thermal fatigue resistance: shot peening, nitriding, "duplex treatment" (TiN onto nitriding or shot peening) and the multilayer with a thin insulating oxide coating. This ranking does not take into account: (i) that the corrosion differs according to the material; (ii) the stress generated by shot peening is affected by high temperature exposure, which again the model ignores.

Especially, considering Table 3:

– For plain steel, the lifetime increases if the aluminium velocity decreases, since the thermal profile is less sharp, leading to lower stress. The values of 10 m/s and 0.5 m/s are typical of injection moulding and gravity moulding. The difference of N_f corroborates the practical difference between both processes. In fact, there is no debate in literature concerning the thermal fatigue in gravity moulding.
– Shot peening and nitriding generate compressive residual stress close to the surface, leading to a negative shift of the strain shown in Fig. 5 and subsequent lower mean stress during the cycle. This improves the thermal fatigue resistance, since N_f is very sensitive to $\bar{\sigma}$.
– TiN, TiN/Ti and boriding slightly increase N_f. This can be attributed to a slight shielding effect for the steel: the latter is exposed to slightly less intensive stress cycles at its surface and neither TiN nor boriding are expected to fail before steel with the strains they undergo.
– Further calculations shows that "Ti", which plays the role of a bond coat, is not likely to fail before TiN, reason why no N_f was calculated for the bond coat (Table 1).
– Using an insulating oxide layer potentially increases the steel lifetime, by reducing steel strain amplitude (compare the double arrows $\Delta\varepsilon_{steel}$ on Figs. 5 and 6). However, decreasing the oxide thickness decreases the possible gain, because of a reduction of this effect (Fig. 7). Note that this assumption is valid only if the mechanical properties of the layer are independent of its thickness, and if no other side effect appear, like delamination.
– The oxide layer was assumed not to limit the overall lifetime. The reverse would imply that the σ_u/E value for this material is lower than the corresponding value for zirconia obtained by plasma spray (0.61%). This is not likely to occur, since using PVD is a way to increase the maximum strain that can withstand thermal barrier coatings.
– TiN and the insulating oxide can be permuted without affecting the lifetime.
– The mechanical properties of the nitriding compound layer are often determining in the overall lifetime. To show this, one let σ_u of this layer vary into a typical range, i.e. between 600 and 1400 HV [34], which corresponds to 55 and 74 HRC, respectively. Applying the equation mentioned in [35], specific for the white layer, expressing σ_u as a function of HRC, these values correspond to 1900 and 3300 MPa. N_f is expressed as a function of σ_u within this range in Fig. 8,

Table 2
σ_0 profile for deep surface treatments.

Nitriding (case depth)		Shot peening	
Depth (μm)	σ_0 (MPa)	Depth (μm)	σ_0 (MPa)
[0; 200[	−500	[0; 250[	−600
		[250; 300[	−450
Remaining	0	[300; 350[	20
		Remaining	0

Table 3
Calculated N_f values (italics: with the default parameters, see Section 3).

Material	Parameters	N_f
Untreated steel	Al velocity = 0.5 m/s	80,500
	Default (Al velocity = 10 m/s)	*56,800*
Shot peening/steel	Default	*72,700*
Nitriding without white layer/steel	Default	*74,200*
Fe_2B (boriding)/steel	Default	*60,200*
TiN (PVD)/steel	Default	*57,000*
TiN (PVD)/Ti (PVD)/steel	Default	*57,100*
TiN (PVD)/shot peening/steel	Default	*72,900*
Nitriding with white layer/steel	σ_u in the compound layer	Fig. 8
	Default (σ_u = 3 GPa)	*76,000*
TiN (PVD)/nitriding without white layer/steel	Default	*74,500*
TiN (PVD)/nitriding with white layer/steel	Default	*76,600*
Insulating oxide (PVD)/TiN (PVD)/Ti (PVD)/steel	Effect of the oxide thickness	Fig. 7
	Default (thickness 10 μm)	*81,700*
TiN (PVD)/insulating oxide (PVD)/Ti/steel	Default	*81,700*
Zirconia (thermal spray)/NiCrAlY (thermal spray)/boriding (Fe_2B)/steel	σ_0 = −100 MPa	425,000
	Default (σ_0 = 0)	*15,900*

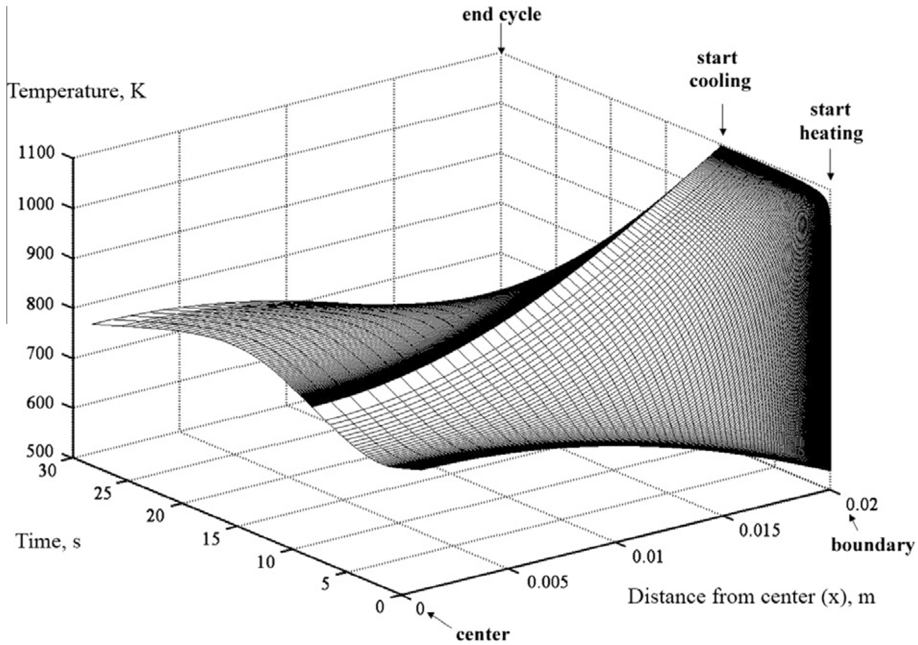

Fig. 4. Temperature (T) as a function of time for one heating/cooling cycle in untreated steel. Only a half thickness is considered.

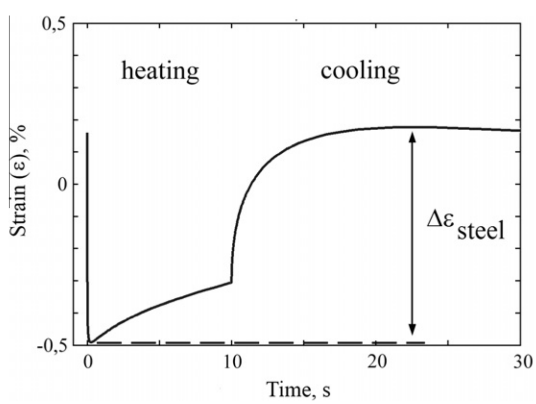

Fig. 5. Surface strain as a function of time for the outermost "slice" of the steel plate (0–10 s: metal introduction; 10–30 s: cooling).

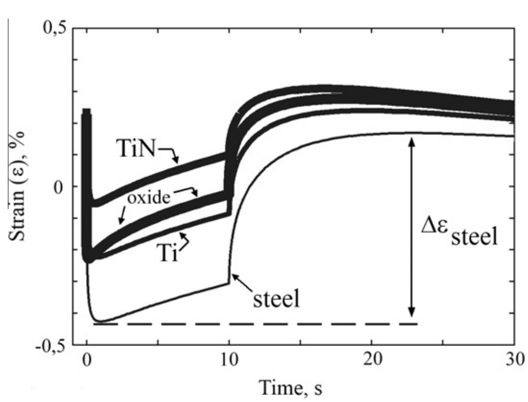

Fig. 6. Strain as a function of time for the multilayer coating: «insulating oxide (PVD)/TiN/Ti/steel», same conditions as Fig. 5.

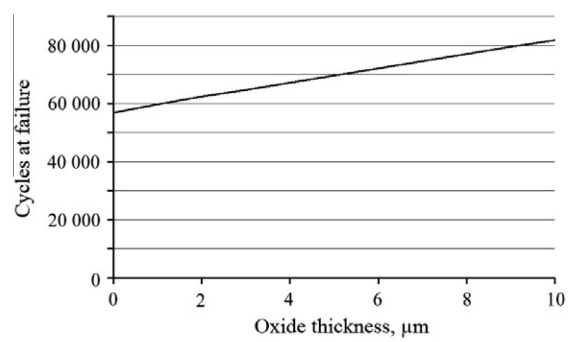

Fig. 7. Effect of the oxide thickness on the number of reversals at failure (N_f), in the multi-layer: insulating oxide (PVD)/TiN/Ti/steel.

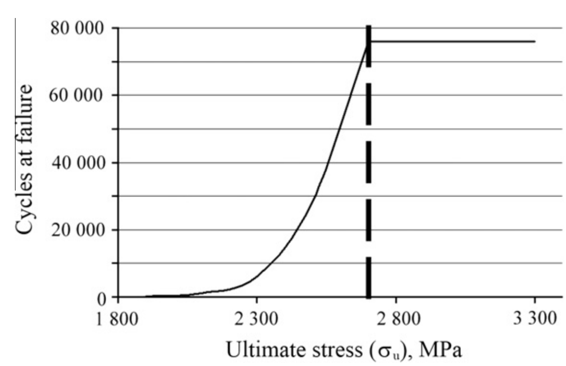

Fig. 8. Effect of the ultimate stress (σ_u) of the nitriding white layer on the number of reversals at failure (N_f).

when all the other parameters remain constant. Under $\sigma_u = 2700$ MPa, σ_u strongly affects the lifetime, because nitriding initiates the failure. This suggests that the operators should take care about the quality of the white layer and may explain the strong difference in thermal fatigue lifetime observed in the presence of a white layer. Peng et al. observe an improvement of lifetime due to nitriding, since the layer they study has $\sigma_u \approx 3000$ MPa [35]. But other authors report worsening thermal fatigue instead.

– The multilayer "Zirconia/NiCrAlY/boriding (Fe_2B)/steel" performs badly, due to the early failure of the zirconia coating. However, this result is very sensitive to residual stress within the coating. Changing them from 0 to $\sigma_0 = -100$ MPa, with E = 10 GPa, increases N_f by more than an order of magnitude. Again, the insulating layer, zirconia, reduces the thermal changes within the substrate. Care is needed if the model is applied to such a material: a strong dispersion in experimental results is expected here because the exponent "-0.083" in Eq. (2) implies that N_f depends on $\Delta\varepsilon^{-12}$ and σ_u^{12}. Accordingly, the behavior of zirconia strongly depends on its processing, the presence of defects and the thermal expansion of the substrate. Besides, specific compressive failure modes are not accounted for in the model. In our previous investigation, the stress in the zirconia layer was generally tensile during the cycles [36]. If the cycles are more shifted to the compressive state, the model may be invalidated.
– In good agreement with the relevant literature [13,25,37], the other studied multi-layers (especially TiN/nitriding/steel and insulating oxide (PVD)/TiN/Ti/steel) are expected to greatly improve the industrial lifetime, since they both improve thermal fatigue resistance (Table 3) and corrosion resistance.

4. Conclusion

A methodology is proposed for a semi-quantitative prediction of the lifetime of surface treated metals in the presence of thermal fatigue. The obtained results can be used as a ranking parameter in an expert system, to compare surface treatments from different technologies. It accounts for the most important parameters usually mentioned in experimental studies of the same kind of problem.

Qualitative observations in the field of foundry moulds were successfully reproduced using this model, especially, the satisfactory response of a duplex-type treatment: PVD nitride layer onto nitriding treatment of steel. The sensitivity to different parameters has been discussed, which might help identify the most critical treatment parameters. The calculations highlight that acting on the internal stress of thick thermal barrier coatings would strongly improve their resistance to the moulding cycles.

Further work should better account for the relaxation of the residual stresses in time during thermal cycling. This implies accessing the parameters of the equations describing this relaxation as a function of time and temperature, for all the studied materials. This cannot be done without considerable experimental work and with a standardized format of the results. More generally, such thermal fatigue problems would be better understood with a wider consensus concerning the measurement of rupture properties of coatings.

Acknowledgements

The authors acknowledge the Walloon Region of Belgium and the European Social Funding for the "First Europe" Grant; Prof. Yves Bréchet (INP Grenoble, France) for a very useful discussion.

References

[1] A.O. Olatunji-Ojo, S.K.S. Boetcher, T.R. Cundari, Comp. Mater. Sci. 54 (2012) 329–335.
[2] M.T. Hernandez, D. Cojocaru, M. Bartsch, A.M. Karlsson, Comput. Mater. Sci. 50 (2011) 2561–2572.
[3] A. Persson, S. Hogmark, J. Bergström, J. Mater. Proc. Technol. 152 (2004) 228–236.
[4] A. Srivastava, V. Joshi, R. Shivpuri, Wear 256 (2004) 38–43.
[5] S.S. Manson, Thermal Stress and Low-cycle Fatigue, MacGraw-Hill, New-York, 1967.
[6] A. Strawbridge, H.E. Evans, Eng. Fail. Anal. 2 (1995) 85–103.
[7] E.S. Puchi-Cabrera, F. Martínez, I. Herrera, J.A. Berríos, S. Dixit, D. Bhat, Surf. Coat. Technol. 182 (2004) 276–286.
[8] Y.L. Su, S.H. Yao, C.S. Wei, W.H. Kao, C.T. Wu, Thin Solid Films 338 (1999) 177–184.
[9] C.M. Suh, B.W. Hwang, R.I. Murakami, Mater. Sci. Eng. A 343 (2003) 1–7.
[10] C.M.D. Starling, J.R.T. Branco, Thin Solid Films 308–309 (1997) 436–442.
[11] V. Joshi, A. Srivastava, R. Shivpuri, Wear 256 (2004) 1232–1235.
[12] V. Joshi, A. Srivastava, R. Shivpuri, E. Rolinski, Surf. Coat. Technol. 163–164 (2003) 668–673.
[13] N. Dingremont, E. Bergmann, P. Collignon, Surf. Coat. Technol. 72 (1995) 157–162.
[14] A. Molinari, M. Pellizzari, G. Straffelini, M. Pirovano, Surf. Coat. Technol. 126 (2000) 31–38.
[15] A. Persson, S. Hogmark, J. Bergström, Surf. Coat. Technol. 191 (2005) 216–227.
[16] M. Pellizzari, A. Molinari, G. Straffelini, Mater. Sci. Eng. A 352 (2003) 186–194.
[17] J.S. Eckersley, J. Champaigne, Shot Peening: Theory and Application, I.I.T.T. International, Gournay s/M, 1991.
[18] C. Mitterer, F. Holler, F. Üstel, D. Heim, Surf. Coat. Technol. 125 (2000) 233–239.
[19] Y. Wang, Surf. Coat. Technol. 94–95 (1997) 60–63.
[20] V.I. Gorokhovsky, D.G. Bhat, R. Shivpuri, K. Kulkarni, R. Bhattacharya, A.K. Rai, Surf. Coat. Technol. 140 (2001) 215–224.
[21] G. Negrea, H. Vermesan, V. Rus, in: 1st International Conference on Heat Treatment and Surface Engineering of Tools and Dies, International Federation for Heat Treatment and Surface Engineering, Pula, 2005, pp. 119–123.
[22] R.H. Biddulph, Thin Solid Films 45 (1977) 341–347.
[23] P. Hairy, R. Dussaussois, Fonderie Fondeur d'Aujourd'hui 227 (2003) 30–41.
[24] D.C. Lou, O.M. Akselsen, M.I. Onsøien, J.K. Solberg, J. Berget, Surf. Coat. Technol. 200 (2006) 5282–5288.
[25] A. Srivastava, V. Joshi, R. Shivpuri, R. Bhattacharya, S. Dixit, Surf. Coat. Technol. 163–164 (2003) 631–636.
[26] T. Yasuda, A. Banno, T. Ito, K. Kiyoshi, K. Ishibayashi, Thermal spraying composite material containing molybdenum boride and a coat formed by thermal spraying, 2001, US patent 6238807.
[27] P. D'Ans, C. Bondoux, C. Degrandcourt, M. Bakrim, J. Dille, L. Segers, M. Degrez, Mater. Sci. Forum 595–598 (2008) 941–950.
[28] J.P. Holman, Heat Transfer, McGraw-Hill, New-York, 1989.
[29] H.J. Lee, S.K. Lee, S.O. Lee, Therm. Conduct. 17 (1983) 229–237.
[30] C.J. Smithells, Metals Reference Book, Butterworths, Londres, 1967.
[31] L.B. Pankratz, J.M. Stuve, N.A. Gokcen, Thermodynamic Data for Mineral Technology, United States Department of the Interior – Bureau of Mines, Avondale, 1984.
[32] O. Kubaschewski, Metallurgical Thermochemistry, Pergamon, Oxford, 1967.
[33] M. Pellizzari, A. Molinari, G. Straffelini, Surf. Coat. Technol. 142–144 (2001) 1109–1115.
[34] M.A. Terres, H. Sidhom, A. Ben Cheikh Larbi, S. Ouali, H.P. Lieurade, Matériaux Techniques 9–10 (2001) 23–36.
[35] W. Peng, X. Wu, Y. Min, L. Xu, in: 6th International Tooling Conference, Karlstads Universitet, Karlstad (Suède), 2002.
[36] P. D'Ans, J. Dille, M. Degrez, Surf. Coat. Technol. 205 (2011) 3378–3386.
[37] J. Walkowicz, J. Smolik, K. Miernik, J. Bujak, Surf. Coat. Technol. 97 (1997) 453–464.
[38] Matweb, database (accessed 08.09).
[39] Handbook of Chemistry and Physics, 47th ed. Chemical Rubber Company, Cleveland, 1966.
[40] V. Ji, Contribution à l'analyse par diffraction des rayons X de l'état microstructural et mécanique des matériaux hétérogènes (habilitation à diriger des recherches), Université des Sciences et Technologies de Lille, Lille, 2003.
[41] T.R. Watkins, R.D. England, C. Klepser, N. Jayaraman, Adv. X-ray Anal. 43 (2000) 31–38.